

## International Journal of Control Theory and Applications

ISSN : 0974-5572

© International Science Press

Volume 10 • Number 34 • 2017

### Advanced Nonlinear Control of Grid Connected Photovoltaicsystem Based on a Half Bridge Inverter

Hajar Dammah, Ibtissam Lachkar\* and Saad Lissane Elhaq\*

<sup>1</sup>Engineering Research Laboratory (LRI), Optimization of Production System & Energy Team University Hassan II, Superior National School of Electricity and Mechanics ENSEM Casablanca, Morocco  
E-mail: hajardammah@gmail.com

**Abstract:** We consider the problem of controlling single-phase grid connected photovoltaic system based on a half bridge inverter. The control objectives are threefold: i) Maximum power point tracking (MPPT) of PV system. ii) Unity power factor in the grid. iii) Regulating the output voltage to a desired reference value. The considered problem is dealt with by designing a nonlinear controller using the sliding mode strategy based on an averaged nonlinear model of the overall controlled system. The system configuration includes a photovoltaic generator, DC-DC converter, DC-AC half bridge inverter coupled to grid. The system is controlling via the input control of the DC-DC converter and DC-AC inverter. The performance of the proposed controller is evaluated through numerical simulation in terms of delivering maximum power and synchronization of grid current with grid voltage under changes in atmospheric conditions. It is easy to shown, that the proposed controller achieves its objectives, through theoretical analysis and simulation results.

**Keywords:** Grid-connected photovoltaic system, Single-phase half-bridge inverter, Maximum power point tracking (MPPT), Unity power factor, Sliding mode strategy.

#### 1. INTRODUCTION

Finally, humanity can be finding a good alternative to surmount problem of producing electrical energy. This alternative is the renewable energy resources especially photovoltaic energy. The most advantage of photovoltaic energy is their high efficiency and low cost. The principle of solar energy is transforming free solar radiation into electricity. Two kind of solution for photovoltaic array is proposed, the first one is the application in stand-alone, this application needs presence of battery, the second one is direct connection to the grid. Grid connected PV system have a low cost but they represent a several technical problems, for example the power of solar array is influenced by radiation and temperature changes, so it's obligatory to design a robust control strategy. In this term it is easy to find many algorithms, for example Perturb & Observe [10], Incremental Conductance [9], fuzzy logic control [11]. Some recent control methods are discussed in [11-20].

The inverter injects excessive harmonic current to the grid. The goal of control is to extract the maximal quantity possible of solar array energy and restitute it to grid with a unity power factor. Photovoltaic grid-

connected system is composed by two-stage. The first stage is a dc-dc converter controlled to meet the MPPT and the second stage is a dc-ac converter controlled to meet unity PF.

In present paper, the focus is controlling a grid connected photovoltaic system based on a half bridge inverter by a nonlinear control based on sliding mode strategy, to track the maximum power of the PV array and to obtain a unity power factor by ensuring the tight regulation of the DC-bus voltage. The half bridge inverter, used in this paper, present many advantage, such as the low cost because reducing of number of interrupters and the current in output is the double compared to the inverter half-bridge. The concept of the control is to calculate an appropriate control law to guarantee the global asymptotic stability of the system. The control input of the DC-DC converter achieves the maximum power point tracking, despite changing of the climatic conditions. The control input of the DC-AC inverter achieves the unity power factor with regulation of the DC-link voltage and assures that the output current must be sinusoidal and in phase with the grid voltage. A theoretical analysis is developed to show that the controller actually meets its objectives a fact that is confirmed by simulation.

The paper is organized as follows: part II describe and model the single phase grid connected PV system. Part III is devoted to controller design and analysis. Part IV illustrates the controller tracking performances by numerical simulation.

## 2. MODELLING OF GRID CONNECTED PV SYSTEM LAYOUT

The single-phase grid connected photovoltaic system under study id represented by Fig.1. It consists of a solar array, a boost dc-dc converter which is used for boosting the PV voltage, a single phase half-bridge inverter (with two IGBT), and a filter inductor  $L_g$ .

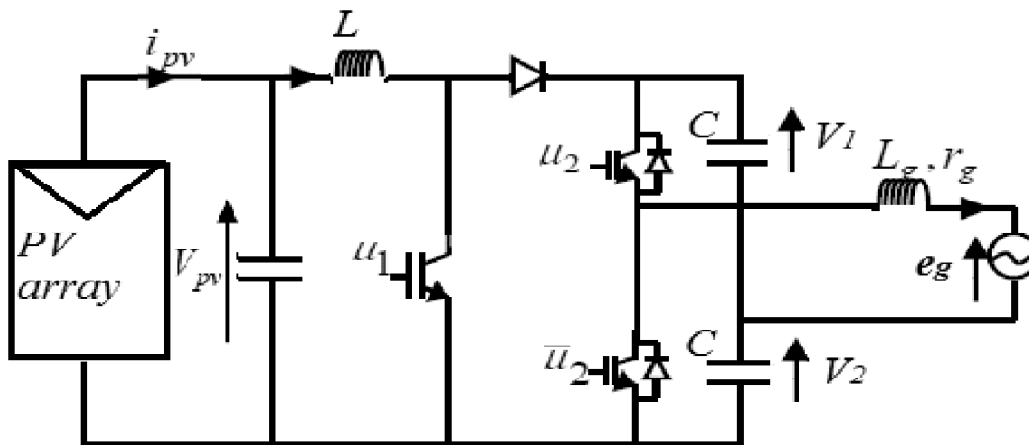


Figure 1: A Single phase grid connected PV system

### 2.1. Photovoltaic Array Model

Equation (1) describes the behavior of the curve for any PV array under different values of temperature and solar irradiance.

$$I_{pv} = N_p I_{ph} - N_p I_o \left\{ \exp \left[ A \left( V_{pv} + \frac{N_s I_{pv} R_s}{N_p} \right) - 1 \right] - \frac{N_p}{R_{sh}} \left( \frac{V_{pv}}{N_s} + \frac{I_{pv} R_s}{N_p} \right) \right\} \quad (1)$$

The meaning and values of the parameters in (1) can be found in many places (see e.g. [1], [2], [3]). The PV array module considered in this paper is the 1STH-215-P. The corresponding electrical characteristics are listed in Table 1.

**Table I**  
Electrical specifications for the solar module 1STH-215P

Parameter	Symbol	Value
Maximum power	Pm	213.15 W
Short circuit current	Isc	7.84 A
Open circuit voltage	Voc	36.3 V
Maximum power voltage	Vm	29 V
Maximum power current	Im	7.35 A
Number of series modules	Ns	6
Number of parallel modules	Np	7

The current-voltage (I-V) and power-voltage (P-V) characteristics under changing temperature are shown in Figure 2 and 3.

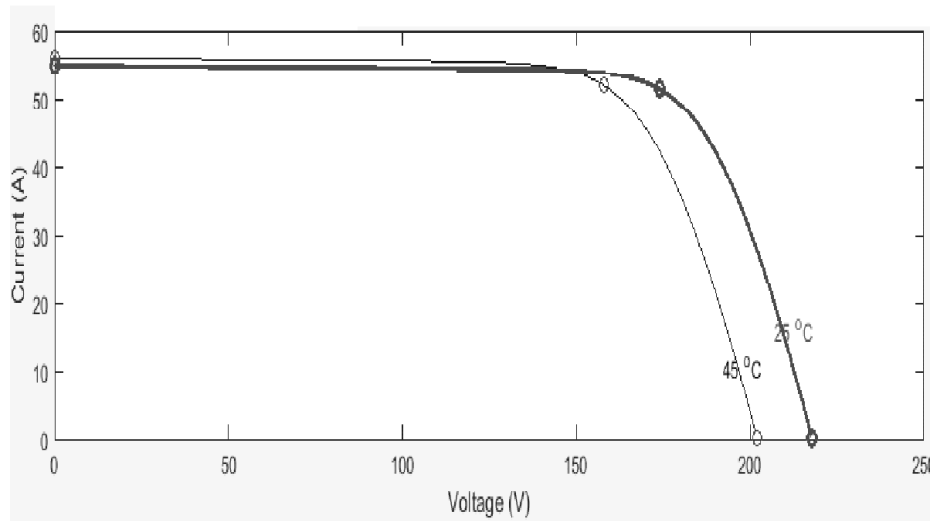


**Figure 2: (I-V) characteristics of The PV module 1STH-215-P with varying temperature**

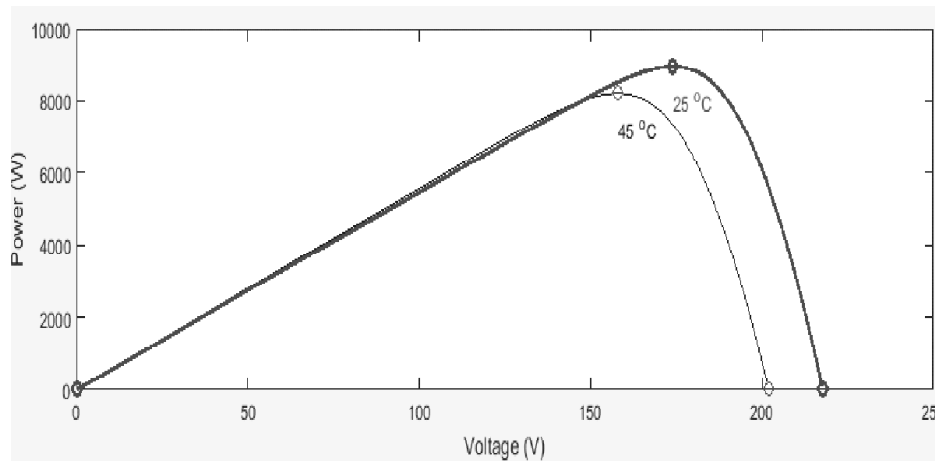


**Figure 3: (P-V) characteristics of The PV module 1STH-215-P with varying temperature**

## 2.2. Boost Converter Modelling

The control input  $u_1$  of the boost converter is a PWM signals with values in the set  $\{0,1\}$ . Applying the Kirchoff's laws to the boost converter presented in figure1, one obtains the following instantaneous model;

$$C_{pv} \frac{dv_{pv}}{dt} = i_{pv} - i_l \quad (2a)$$

$$L \frac{di_l}{dt} = v_{pv} - (1-u_1)(v_1 + v_2) \quad (2b)$$

## 2.3. Single Phase Half-bridge Inverter Modelling

The control input  $u_2$  for the single-phase half-bridge inverter is also a PWM signal taking values in the set  $\{-1,1\}$ . Applying the Kirchoff's laws, to the inverter circuit of Fig. 2 one obtains the following instantaneous model:

$$C \frac{dv_1}{dt} = (1-u_1)i_l - \frac{u_2+1}{2}i_g \quad (3a)$$

$$C \frac{dv_2}{dt} = (1-u_2)i_l - \frac{u_2-1}{2}i_g \quad (3b)$$

$$L_g \frac{di_g}{dt} = -r_g i_g + \frac{1+u_2}{2}v_1 - \frac{1-u_2}{2}v_2 - e_g \quad (3c)$$

With  $r_g$  is the equivalent series resistance of inductance  $L_g$ .

## 2.4. Overall System Model

Performing a following transformation

$$v_1 + v_2 = v_o ; v_1 - v_2 = v_d$$

Combining systems of equation (2) et (3), the model comes:

$$C_{pv} \frac{dv_{pv}}{dt} = i_{pv} - i_l \quad (4a)$$

$$L \frac{di_l}{dt} = v_{pv} - (1-u_1)v_o \quad (4b)$$

$$C \frac{dv_o}{dt} = 2(1-u_1)i_l - u_2 i_g \quad (4c)$$

$$C \frac{dv_d}{dt} = -i_g \quad (4d)$$

$$L_g \frac{di_g}{dt} = -r_g i_g + \frac{v_d}{2} + \frac{u_2}{2} v_o - e_g \quad (4e)$$

This model cannot be based upon to design a continuous control law as it involves a binary control input,  $u_1$  and  $u_2$ . To overcome this difficulty, it is usually resorted to the averaging model [7].

$$C_{pv} \frac{dx_1}{dt} = \bar{i}_{pv} - x_2 \quad (5a)$$

$$L \frac{dx_2}{dt} = x_1 - (1 - \mu_1)x_3 \quad (5b)$$

$$C \frac{dx_3}{dt} = 2(1 - \mu_1)x_2 - \mu_2 x_5 \quad (5c)$$

$$C \frac{dx_4}{dt} = -x_5 \quad (5d)$$

$$L_g \frac{dx_5}{dt} = -r_g x_5 + \frac{x_4}{2} + \frac{\mu_2}{2} x_3 - e_g \quad (5e)$$

**Table II**  
Model Averaged Values

Physical variable	Averaged values
PV voltage $v_{pv}$	$x_1$
Inductor current $i_l$	$x_2$
Sum of Voltage $v_o$	$x_3$
Difference of Voltage $v_d$	$x_4$
Grid current $i_g$	$x_5$
PV current $i_{pv}$	
Converter binary control input $u_1$	$\mu_1$
Inverter binary control input $u_2$	$\mu_2$

### 3. CONTROLLER DESIGN

The objective of this section is to be able to ensure: (i) a perfect MPPT whatever the position of the panel, the controller must enforce the voltage  $x_1$  to track the optimal voltage  $V_m$  which depend on temperature and solar variation  $I_r$ . (ii) a unity PF in the grid. (iii) a tight regulation of the voltage  $x_3$ .

#### 3.1. Maximum Power Point Tracking Objective

The goal, in this part, is to enforce the voltage  $x_1$  to track the optimal voltage  $V_m$ . The regulator will be designed using the nonlinear control based on sliding mode strategy [8].

Considering the sub-system (5a-b):

$$C_{pv} \frac{dx_1}{dt} = \bar{i}_{pv} - x_2 ;$$

$$L \frac{dx_2}{dt} = x_1 - (1 - \mu_1)x_3$$

Let us introduce the following sliding manifold:

$$s_1 = \dot{e}_1 + c_1 e_1 \tag{6}$$

with  $c_1$  is a positive design parameter and  $e_1$  is the tracking error

$$e_1 = x_1 - V_m \tag{7}$$

The algorithm of control can be defined as follow:

$$\mu_1 = \mu_{1eq} + \mu_{1N} \tag{8}$$

With  $\mu_{1eq}$  is the equivalent control law, it consist to find a continuous value of the control variable such as state vector trajectory is maintained on the sliding surface  $s(t) = 0$ . And  $\mu_{1N}$  is the discontinuous component.

The Equivalent control law is a way to determine the system performance when restricted to the surface  $s(t) = 0$ , which implies  $\dot{s}(t) = 0$ , so the equivalent control law is:

$$\mu_{1eq} = 1 - \left( \frac{x_1 - L\dot{i}_{pv} + C_{pv}L\ddot{V}_m - c_1L(i_{pv} - x_2)}{x_3} + \frac{c_1C_{pv}L\dot{V}_m}{x_3} \right) \tag{9}$$

The convergence condition is defined by the Lyapunov function, it makes the surface attractive and invariant, then  $s(t)\dot{s}(t) < 0$ . This condition will be satisfied if

$$\mu_{1N} = -K_1 \text{sign}(s) \tag{10}$$

with  $K_1$  a positive constant and the signe function is defined like as:

$$\begin{aligned} \text{sign}(s(t)) &= 1 \quad \text{if } s(t) > 0 \\ \text{sign}(s(t)) &= 0 \quad \text{if } s(t) = 0 \\ \text{sign}(s(t)) &= -1 \quad \text{if } s(t) < 0 \end{aligned}$$

Combining (9) and (10), the control law of the boost controller is:

$$\mu_1 = 1 - \left( \frac{x_1 - L\dot{i}_{pv} + C_{pv}L\ddot{V}_m - c_1L(i_{pv} - x_2)}{x_3} + \frac{c_1C_{pv}L\dot{V}_m}{x_3} \right) - K_1 \text{sign}(s) \tag{11}$$

### 3.2. Algorithm for Generation the Optimal Voltage VM

The voltage and current delivered by the PV array are affected by the not stable climate conditions. There are several algorithms to search the optimal point (see [4],[5],[6]). On this paper the P&O algorithm is used:

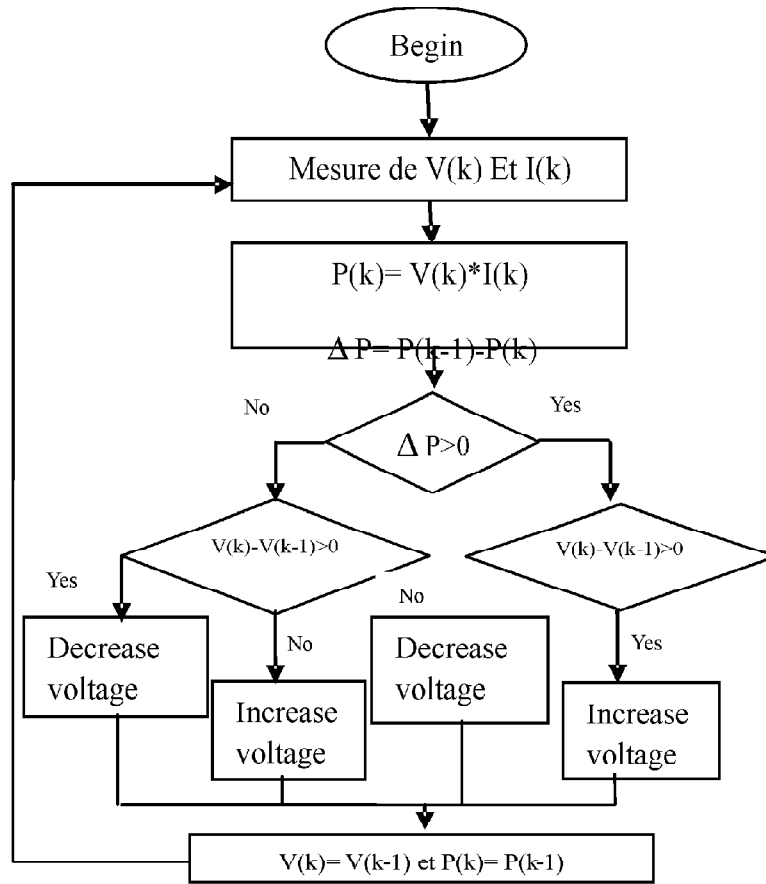


Figure 4: Algorithm perturb and observe

### 3.2. Power Factor Unity Objective

#### 3.2.1. Current Inner Loop Design

In this section we are invited to satisfied the PFC objective, it means that the converter output current must be sinusoidal and in phase with the grid voltage  $e_g$ . The regulator should be enforces the current  $x_5$  to track a reference signal of the form

$$x_5^* = \beta e_g \quad (12)$$

The nonlinear sliding mode control is used to design the regulator. Let us introduce the following current error:

$$e_2 = L_g (x_5 - x_5^*) \quad (13)$$

The degree of system is 1. So the sliding surface is defined as follow  $s_2 = e_2$ .

The equivalent control law is:

$$\mu_{2eq} = 2 \frac{L_g \dot{x}_5^* + e_g - \frac{x_4}{2} + r_g x_5}{x_3} \quad (14)$$

The discontinuous component is defined during the convergence phase like as:

$$\mu_{2N} = -K_2 \text{sign}(s) \tag{15}$$

With  $K_2$  is a positive parameter.

Combining (14) and (15) one gets the following control law  $\mu_2$ :

$$\mu_2 = 2 \frac{L_g \dot{x}_5^* + e_g - \frac{x_4}{2} + r_g x_5}{x_3} - K_2 \text{sign}(s) \tag{16}$$

### 3.2.2. Outer Voltage Loop Design

The aim of this outer loop is to generated a variation law for the ratio  $\beta$  in such that the voltage  $v_o$  be regulated to his reference value

$$\beta = G_2(s) \xi_{dc} \tag{17a}$$

$$G_2(s) = k_p + \frac{k_i}{s} \tag{17b}$$

$$\xi_{dc} = x_3 - V_{oref} \tag{17c}$$

Theorem (main result). Consider the single-phase grid-connected PV system shown in Figure.2, represented by its average model (5a-e), together with the controller consisting of the control laws (10), (16) and (17a-c). Then, one has the following results:

- i) The system is brought to the surface  $s_1$  and maintained on, implying the MPPT achievement.
- ii) The system is brought to the surface  $s_2$  and maintained on, ensuring a unity PF.
- iii) The tracking error  $\xi_{dc}$  converges to zero guaranteeing a tight regulation of the dc bus voltage.

## 4. SIMULATION

To illustrate the performances of regulators previously established, we developed simulators, with Matlab/Simulink environment. The characteristics of the controlled system are listed in Table III. The control design parameters are given values of Table IV which proved to be convenient. The resulting closed-loop control performances are illustrated by Figure 6 to Figure 9.

**Table III**  
Characteristics of controlled system

Parameter	Symbol	Value
DC/AC converter	Power	213.15W
	Modul	1STH-215-P
	L	2mH
	Cpv	4mF
	C	4mF
	Lg	10mH
PWM	rg	0.7&!
	Switching frequency	10kHz
	AC Source	220V
	Frequency	50Hz



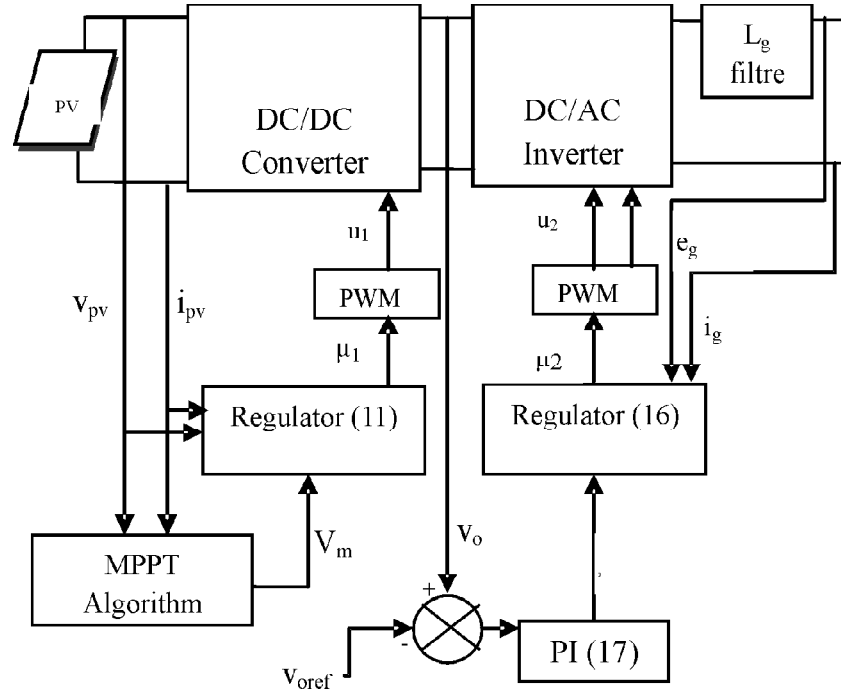


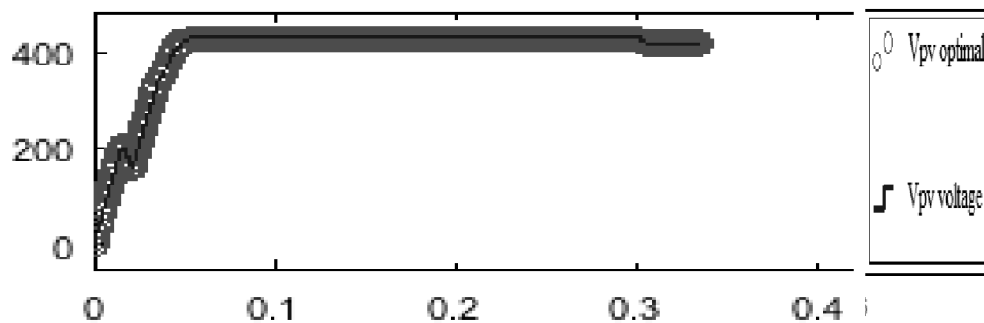
Figure 4: Control structure

Table IV  
controller parameter

Parameter	Symbol	Value
Regulator U2	c1	0.25
	K1	1e4
	K2	1e14
	kp	1e-6
	ki	4e-7
Desired vo voltage	voref	1000V

#### 4.1. Radiation Change Effect

Fig. 6 shows that the PV voltage converges to its reference with good accuracy ensuring the perfect MPPT in presence of radiation changes. Specifically, the radiation varies between 400 W/m<sup>2</sup> and 1000 W/m<sup>2</sup> at 0.3s, meanwhile the temperature is kept constant, equal to 298.15K (i.e. 25°C). The figure, also shows that the DC bus voltage vo is regulated to its desired value. Fig. 7 shows that the grid current ig is sinusoidal and therefore demonstrates the good performance of the inner loop.



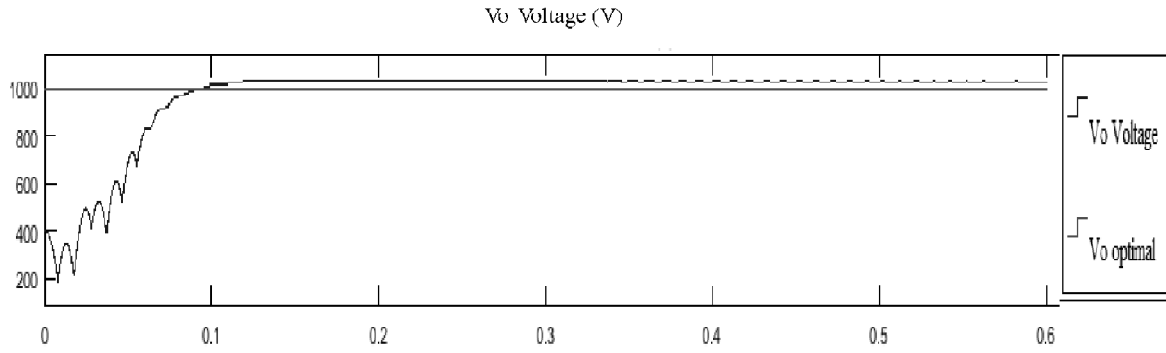
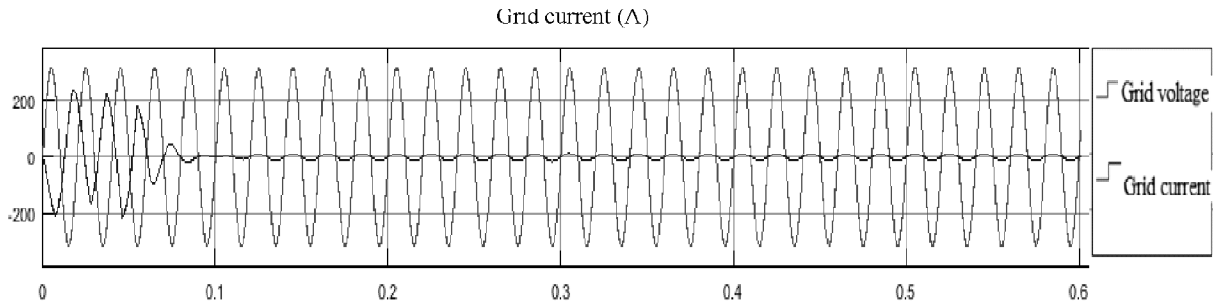


Figure 6: MPPT & Vo voltage in presence of radiation change



#### 4.1. Temperature Change Effect

From Fig. 9, it is clear that the maximum power point is reached with excellent accuracy and good performances according to temperature changes. Specifically, the temperature  $T$  varies between  $25^{\circ}\text{C}$  and  $35^{\circ}\text{C}$  at  $0.3\text{s}$ , while the radiation maintained constant at  $1000\text{W}/\text{m}^2$ . Noting that the DC bus voltage is regulated to its desired value  $v_{\text{oref}}$ . The last figure shows clearly that the grid current  $i_g$  is sinusoidal and in phase with the grid voltage  $e_g$ , which proves the unity power factor achievement.

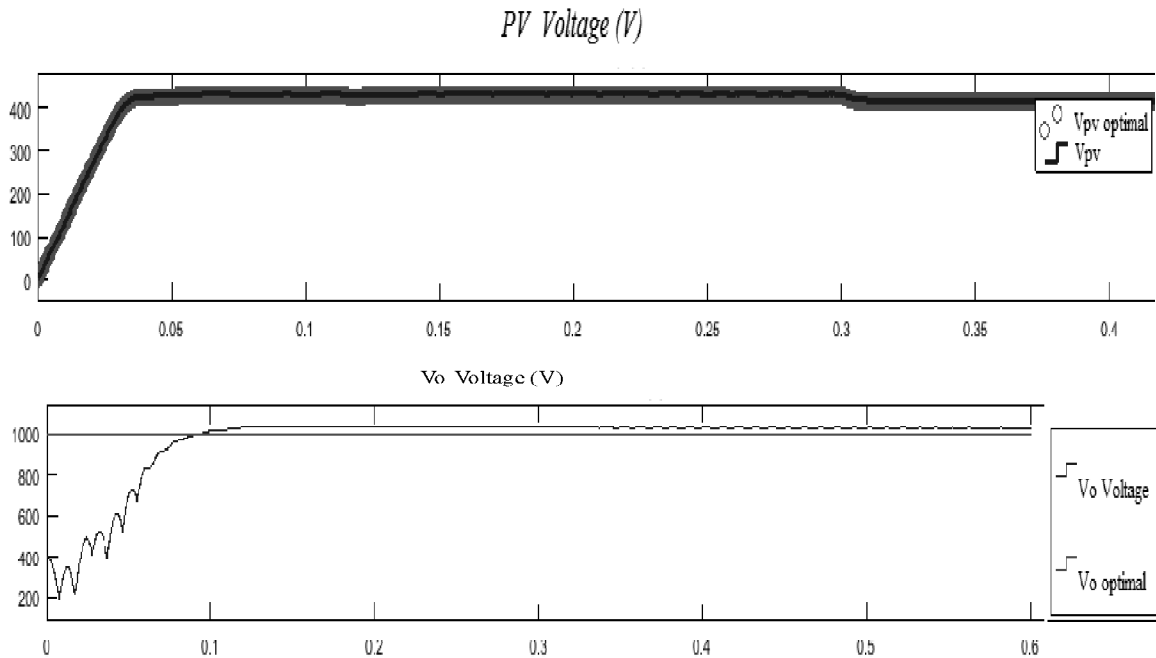


Figure 9: MPPT & Vo voltage in presence of temperature change

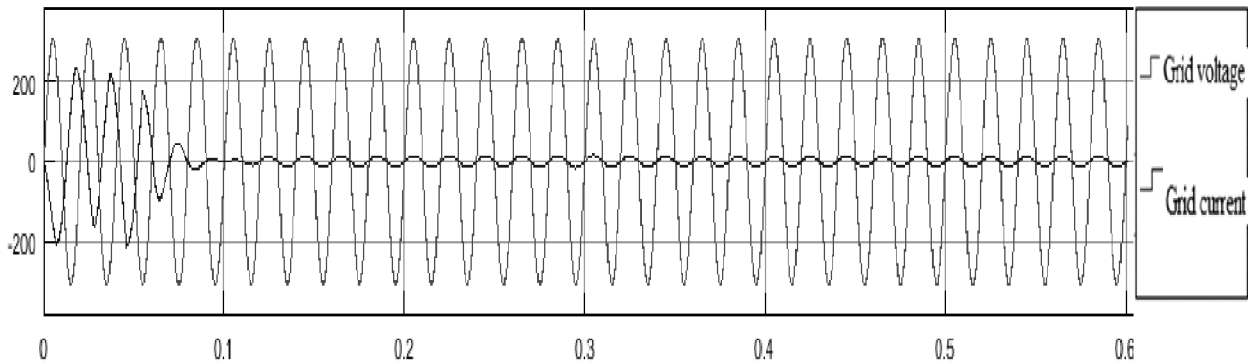


Figure 10: Unity PF in presence of temperature changes

## 5. CONCLUSIONS

In this paper, a new nonlinear control strategy has been presented using sliding mode design strategy, based on the nonlinear model (5a-e). The controller is designed to obtain the MPPT, inject a sinusoidal current in the grid with unity PF and regulate the DC bus voltage. To control system, two sliding mode controllers are developed to extract the law control for converter and inverter (11) & (16), and a proportional-integral controller to regulate the DC voltage (17a-c). The present controller has the advantage such as robustness against changes in system parameters, and insensitivity to external perturbations. Both analysis and simulation studies prove that the proposed controllers meet the objectives.

## REFERENCES

- [1] C. Chen-Chi, C. Chieh-Li. "Robust maximum power point tracking method for photovoltaic cells: A sliding mode control approach". *Solar Energy*, 83, 1370–1378, 2009.
- [2] H. El Fadil, and F. Giri, "Climatic sensorless maximum power point tracking in PV generation systems". *Control Engineering Practice*, 19 (5), 513–521, May 2011.
- [3] J.M. Enrique, E. Duran, M. Sidrach-de-Cardona and J.M. Andujar. "Theoretical assessment of the maximum power point tracking efficiency of photovoltaic facilities with different converter topologies". *Solar Energy*, 81, 31-38, 2007.
- [4] H.N. Zainudin and S. Mekhilef, "Comparison Study of Maximum Power Point Tracker Techniques for PV Systems ". Proceedings of the 14th International Middle East Power Systems Conference (MEPCON'10), Cairo University, Egypt, December 19-21, 2010.
- [5] H. Abbes, H. Abid, K. Loukil, A. Toumi and M. Abid, "Etude comparative de cinq algorithmes de commande MPPT pour un système photovoltaïque". Conférence Internationale des Energies Renouvelables (CIER'13), Sousse, Tunisie, 2013.
- [6] C. Hua, J. Lin and H. Tzou. "MPP control of a photovoltaic energy system." *EPEP* 13 (4), July/August 2003.
- [7] P.T. Krein, J. Bentsman, R.M. Bass, and B. Lesieutre, "On the use of averaging for analysis of power electronic system". *IEEE Transactions on Power Electronics*, 5(2), pp. 182–190, 1990.
- [8] V.I Utkin, "Variable structure systems with sliding mode". *IEEE transactions on Automatic Control*, 22 (2), 212-222, 1977.
- [9] J.H. Lee, H.S. Bae and B.H. Cho, "Advanced Incremental Conductance MPPT Algorithm with a Variable Step Size", *12<sup>th</sup> International Power Electronics and Motion Control Conference*, pp. 603 – 607, Sept 2006.
- [10] N. Femia, G. Petrone, G. Spagnuolo, and M. Vitelli, "Optimization of Perturb and Observe maximum power point tracking method", *IEEE Transactions on Power Electronics*, 20 (4), 963-973, 2005.
- [11] N. Patcharaprakiti, S. Premrudeepreechacharn and Y. Sriuthaisiriwong, "Maximum power point tracking using adaptive fuzzy logic control for grid-connected photovoltaic system", *Renewable Energy*, 30 (11), 1771-1778, 2005.

- [12] A.T. Azar and S. Vaidyanathan, *Chaos Modeling and Control Systems Design*, Springer, Berlin, 2015.
- [13] S. Vaidyanathan, "A novel 3-D conservative chaotic system with sinusoidal nonlinearity and its adaptive control", *International Journal of Control Theory and Applications*, 9 (1), 115-132, 2016.
- [14] S. Vaidyanathan and S. Pakiriswamy, "A five-term 3-D novel conservative chaotic system and its generalized projective synchronization via adaptive control method", *International Journal of Control Theory and Applications*, 9 (1), 61-78, 2016.
- [15] V.T. Pham, S. Jafari, C. Volos, A. Giakoumis, S. Vaidyanathan and T. Kapitaniak, "A chaotic system with equilibria located on the rounded square loop and its circuit implementation," *IEEE Transactions on Circuits and Systems-II: Express Briefs*, 63 (9), 2016.
- [16] S. Vaidyanathan and S. Sampath, "Anti-synchronisation of identical chaotic systems via novel sliding control and its application to a novel chaotic system," *International Journal of Modelling, Identification and Control*, 27 (1), 3-13, 2017.
- [17] S. Vaidyanathan, K. Madhavan and B.A. Idowu, "Backstepping control design for the adaptive stabilization and synchronization of the Pandey jerk chaotic system with unknown parameters," *International Journal of Control Theory and Applications*, 9 (1), 299-319, 2016.
- [18] R.K. Goyal, S. Kaushal and S. Vaidyanathan, "Fuzzy AHP for control of data transmission by network selection in heterogeneous wireless networks," *International Journal of Control Theory and Applications*, 9 (1), 133-140, 2016.
- [19] C.K. Volos, D. Prousalis, I.M. Kyrianiadis, I. Stouboulos, S. Vaidyanathan and V.T. Pham, "Synchronization and anti-synchronization of coupled Hindmarsh-Rose neuron models," *International Journal of Control Theory and Applications*, 9 (1), 101-114, 2016.
- [20] S.M.B. Mansour and V. Sundarapandian, "Design and control with improved predictive algorithm for obstacles detection for two wheeled mobile robot navigation," *International Journal of Control Theory and Applications*, 9 (38), 37-54, 2016.